SECURITY CLASSIFICATION OF THIS PAGE (When Data Entered)

REPORT DOCUMENTATION PAGE

READ INSTRUCTIONS BEFORE COMPLETING FORM

1. REPORT NUMBER: Annual Technical Report	2. GOVT ACCESSION NO.
3. RECIPIENT'S CATALOG NUMBER: ADA203038	
4. TITLE (and Subtitle): High Temperature Oxidation and Electrochemical Studies Related to Hot Corrosion	5. TYPE OF REPORT & PERIOD COVERED: Annual Technical Report
	6. PERFORMING ORG. REPORT NUMBER
7. AUTHOR(s): D-H. Kim, R. F. Reidy and G. Simkovich	8. CONTRACT OR GRANT NUMBER(s): N0014-86-K-0133
9. PERFORMING ORGANIZATION NAME AND ADDRESS: Metals Science & Eng., 209 Steidle Building, The Pennsylvania State University, University Park, PA 16802	10. PROGRAM ELEMENT, PROJECT, TASK AREA & WORK UNIT NUMBERS
11. CONTROLLING OFFICE NAME AND ADDRESS: Metallurgy Branch, Office of Naval Research, Arlington, VA 22217	12. REPORT DATE
	13. NUMBER OF PAGES
14. MONITORING AGENCY NAME & ADDRESS (if different from Controlling Office)	15. SECURITY CLASS. (of this report)
	15a. DECLASSIFICATION/DOWNGRADING SCHEDULE

16. DISTRIBUTION STATEMENT (of this Report)

17. DISTRIBUTION STATEMENT (of the abstract entered in Block 20, if different from Report)

18. SUPPLEMENTARY NOTES

19. KEY WORDS (Continue on reverse side if necessary and identify by block number)

20. ABSTRACT (Continue on reverse side if necessary and identify by block number)

In order to aid in further understanding hot corrosion processes, investigations of the electrical behavior of molten Na_2SO_4 have been undertaken. Wagner-Hebb type polarization experiments and total electrical conductivity measurements by an A.C. impedance technique were carried out on melts of Na_2SO_4, both pure and those containing 10^{-3} m/o, 1.8×10^{-1} m/o, and supersaturated (10 m/o) NiO, as a function of Na_2O activity at 1173 K. Additionally, the relative contributions of cation versus anion transport in the molten sodium sulfate was investigated by employing a potentiostatic polarization technique.

DD FORM 1 JAN 73 1473 EDITION OF 1 NOV 65 IS OBSOLETE
S/N 0102-014-6601

SECURITY CLASSIFICATION OF THIS PAGE (When Data Entered)

It was observed that the total electrical conductivity of pure Na_2SO_4 was of the order of 2.57×10^{-1} $(ohm\text{-}cm)^{-1}$ and varied only slightly with changes in the activity of Na_2O. From the Wagner-Hebb type D.C. polarization experiments on pure Na_2SO_4, the electron conductivity was shown to be much greater than the electron hole conductivity over the entire range of Na_2O activities. The partial conductivity of electrons in Na_2SO_4 was about three orders of magnitude less than the total electrical conductivity. Thus, transport number of electrons, t_θ, is of the order of 10^{-4} in a pure Na_2SO_4 melt at 1173 K. From the potentiostatic polarization technique, the cation transport number of a pure sodium sulfate melt was about 0.86 at 1173 K.

The introduction of NiO into Na_2SO_4 melts at 1173 K did not produce massive changes in the total electrical conductivities of these melts as compared to those of a pure Na_2SO_4 melt. However, the addition of NiO in the melt decreases the electronic conductivities as well as the transport numbers of electronic species, regardless of the concentrations of NiO in the melt at 1173 K.

ABSTRACT

In order to aid in understanding hot corrosion processes, investigations of the electrical behavior of molten Na_2SO_4 have been undertaken. Wagner-Hebb type polarization experiments and total electrical conductivity measurements by an A.C. impedance technique were carried out on melts of Na_2SO_4, both pure and those containing 10^{-3} m/o, 1.8×10^{-1} m/o, and supersaturated (10 m/o) NiO, as a function of Na_2O activity at 1173 K. Additionally, the relative contributions of cation versus anion transport in the molten sodium sulfate was investigated by employing a potentiostatic polarization technique.

It was observed that the total electrical conductivity of pure Na_2SO_4 was of the order of 2.57×10^{-1} (ohm-cm)$^{-1}$ and varied only slightly with changes in the activity of Na_2O. From the Wagner-Hebb type D.C. polarization experiments on pure Na_2SO_4, the electron conductivity was shown to be much greater than the electron hole conductivity over the entire range of Na_2O activities. The partial conductivity of electrons in Na_2SO_4 was about three orders of magnitude less than the total electrical conductivity. Thus, transport number of electrons, t_θ, is of the order of 10^{-4} in a pure Na_2SO_4 melt at 1173 K. From the potentiostatic polarization technique, the cation transport number of a pure sodium sulfate melt was about 0.86 at 1173 K.

The introduction of NiO into Na_2SO_4 melts at 1173 K did not produce massive changes in the total electrical conductivities of these melts as compared to those of a pure Na_2SO_4 melt. However, the addition of NiO in the melt decreases the electronic conductivities as well as the transport numbers of electronic species, regardless of the concentrations of NiO in the melt at 1173 K.

I. INTRODUCTION

Hot corrosion is generally defined in broad terms as an accelerated or catastrophic oxidation of alloys and other materials. This form of attack is particularly severe in the temperature range of 1033 - 1273 K and it has affected both aircraft engines and industrial gas turbines. There is a general agreement that condensed alkali metal salts, notably Na_2SO_4, are a prerequisite to hot corrosion. The source of this salt may be (a) the direct ingestion of sea salt in a marine environment, (b) the formation of Na_2SO_4 during combustion of fuels containing both sodium and sulfur, (c) the formation of Na_2SO_4, during combustion, from sodium - contaminated, airborne dust and sulfur in the fuel [1].

The exact mechanisms of hot corrosion are still uncertain, but from many studies on the hot corrosion mechanisms of metals and alloys, the various mechanisms that have been proposed can be broadly classified into two categories : (a) acidic - basic fluxing models [2-4] and (b) dissolution - reprecipitation electrochemical model [5]. The overall mechanisms of hot corrosion involve the dissolution of normally protective oxide layers and the formation of porous, nonadherent, and hence unprotective scales when alloy surfaces are covered by a thin film of liquid sodium sulfate. It appears that the initial formation of metal oxides is necessary for the initial reaction and the transport of oxygen through the molten salt phase is required to form such metal oxides.

Little is known about the electronic transport properties in molten Na_2SO_4. This study is, therefore, concerned with obtaining such information to aid in the elucidation of the mechanism of the process. A potentiostatic polarization technique was employed to estimate the ionic transport numbers of a pure sodium sulfate melt at 1173 K. The electronic conductivities by Wagner-Hebb type polarization studies [6,7] as well as total electrical conductivity measurements by an A.C. impedance technique were carried out on molten Na_2SO_4 as a function of Na_2O activities at 1173 K since the proposed models

which describe the degradation behavior of alloys are strongly dependent on SO_2, O_2, and /or SO_3 gas pressure, i.e., the Na_2O activity in the Na_2SO_4 deposit. The transport numbers of electronic species in Na_2SO_4 melt were evaluated by dividing the values of electronic conductivities by those of total electrical conductivities. Additionally, such studies were conducted in molten Na_2SO_4 containing NiO to elucidate the effect of NiO on the transport mechanism in the Na_2SO_4 melt at 1173 K.

II. THEORETICAL BACKGROUND

(i) Total Conductivity Measurement

A.C. impedance measurements were conducted to obtain polarization free total electrical conductivity of molten sodium sulfate and the melts containing NiO. In D.C. techniques, a space charge of either ions or electrons form in the vicinity of the electrodes, which leads to a non-uniform field across the specimen. However, in A.C. impedance techniques, the use of small amplitude sinusoidal potentials does not disturb the electrode properties and at higher frequencies polarization at the specimen electrode may be eliminated. Thus, an A.C. impedance technique was utilized to measure the resistance of a pure Na_2SO_4 melt and melts containing NiO since the melts showed some polarization effects at the electrodes in our preliminary D.C. experiments.

Impedance can be thought of as the resistance of a circuit to an alternating waveform; as opposed to a pure resistance it has not only magnitude but also direction - phase angle. One of the advantages of A.C. impedance techniques over conventional D.C. electrical conductivity efforts is the ability to separate the real and imaginary components of impedance. An impedance, Z, can be completely defined by specifying the magnitude, $|Z|$, and the angle, ϕ, or alternatively by specifying the magnitude of its real , Z', and imaginary, Z", components [8].

There are a number of graphical interpretations available for impedance data analysis over a wide frequency range [9]. A plot of Z' versus wZ" was employed to evaluate the resistance of the molten salts. A plot of Z' versus wZ" shows a straight line with a slope of $-R_pC$ and an intercept of $R\Omega + R_p$ according to the following equation:

$$Z' = R_\Omega + R_p - R_p C w Z'' \qquad (2.1)$$

where
- Z' is the real part of the impedance
- Z" is the imaginary part of the impedance
- $R\Omega$ is the resistance of the electrolyte
- R_p is the polarization resistance
- C is the capacitance
- w is angular frequency ($= 2\pi f$)

The real and imaginary part of the impedance can be expressed by the following relationship [10].

$$Z' = R_\Omega + \frac{R_p}{1 + w^2C^2R_p^2} \qquad (2.2)$$

$$Z'' = \frac{wCR_p^2}{1 + w^2C^2R_p^2} \qquad (2.3)$$

Thus, as frequency increases the straight line of a plot of Z' versus wZ" levels off and the projection of this point onto the Z' axis affords the sum of the resistances of the electrolyte and the circuit leads according to the equation (2.2).

(ii) Electronic Conductivity Measurement

The idea that an appropriate choice of electrodes enables the suppression of either ionic or electronic transport in a galvanic cell provides the basis for the polarization technique. This technique has been extensively employed to investigate electronic conductivity in ionic solids [11-16] and has also been applied to a few molten systems [17-19].

Wagner [6] has derived the appropriate relation for the polarization conditions from transport theory. This relation states that, under steady state conditions, the total current due to passage of electronic species through the polarization cell is given by

$$I_{elect} = I_{\theta} + I_{\oplus}$$

$$= \frac{RTA}{LF}\left\{ \sigma^{o}_{\theta}\left[1-\exp\left(-\frac{EF}{RT}\right)\right] + \sigma^{o}_{\oplus}\left[\exp\left(\frac{EF}{RT}\right) - 1\right]\right\} \qquad (2.4)$$

where $I_{\theta}, I_{\oplus}$: electron and electron hole currents, respectively

$\sigma_{\theta}^{o}, \sigma_{\oplus}^{o}$: electron and electron hole conductivity, respectively

E : applied voltage

F : Faraday constant

R : gas constant

T : temperature (K)

L/A : cell constant.

In the derivation of equation (2.4) it is assumed [18,19] that

(i) excess electrons and holes follow the laws of ideal dilute solutions,

(ii) their mobilities are independent of concentrations,

(iii) the change in the concentration of atomic defects arising from thermal disorder with variation in the metal to nonmetal ratio is small,

(iv) convection in the melt is negligible.

The division of equation (2.4) by [1-exp(-EF/RT)] and rearrangement gives

$$I_{elect}\left\{\frac{LF}{RTA}\left[\frac{1}{1-\exp\left(-\frac{EF}{RT}\right)}\right]\right\} = \sigma_{\theta}^{o} + \sigma_{\oplus}^{o}\exp\left(\frac{EF}{RT}\right) \qquad (2.5)$$

and a plot of the left hand side of equation (2.5) versus exp (EF/RT) gives $\sigma\theta^{\circ}$ as the intercept and $\sigma\oplus^{\circ}$ as the slope. These values, combined with total electrical conductivity results, permit the evaluation of the transport numbers of each electronic carrier in the molten salts.

In the present work, D.C. current flowing through the polarization cell is measured at various applied voltages, which are kept below the decomposition potentials of the sample to ensure that the measured current is only the electronic current.

(iii) Evaluation of Ionic Transport Numbers

The potentiostatic polarization cell technique was employed to determine ionic transport numbers for molten sodium sulfate at 1173 K. In a recent application of this technique reasonable agreement was obtained with transport numbers from Tubandt and tracer diffusion techniques [20]. This technique is based on a two electrode cell. A constant D.C. potential is applied by a potentiostat and the current is monitored as a

function of time. The electrode is chosen to be reversible with respect to the cation present in the electrolyte.

Under the influence of a D.C. field cations migrate to the negative electrode and anions to the positive electrode. As the concentration of anions increases near the positive electrode, local charge neutrality requires that a cation accompany each anion. This process establishes a salt concentration gradient across the electrolyte. As the cell polarizes the amount of current carried by the anion decreases but the amount carried by the cation remains constant. When the back potential created by the concentration gradient exactly opposes the applied potential the anions no longer carry current and the cell is completely polarized with respect to the anion. Thus, the ratio of final current, due to the cation only, to the initial current, due to the cation and anion, yields the cation transport numbers of molten Na_2SO_4.

III. EXPERIMENTAL PROGRAM

(i) Gas Control

Variations on our previous measurements [21] was performed. In particular instead of using the SO_2/O_2 obtained by flowing helium over a $ZnO/ZnSO_4$ mixture mass flow control meters (MKS Model 1259B) coupled with 4 channel readout (MKS Type 247C) was utilized for better control of SO_2/O_2 ratios.

(ii) A.C. Impedance Measurements

A.C. impedance measurements were performed to obtain polarization free total electrical conductivity. As shown in Figure 1, the three electrode system was utilized for the A.C. impedance measurements. The reference electrode was a silver wire immersed into a 10 m/o Ag_2SO_4/Na_2SO_4 melt contained in the Na ion conducting membrane, mullite

tube (0.7 cm O.D.) [22]. Pure gold wires serve as the working electrode and counter electrode. Platinum wires welded to those electrodes were employed as leads to connect to the EG & G Model 273 potentiostat coupled with Model 5208 Lock-In amplifier. The schematic arrangements for the A.C. impedance measurements are depicted in Figure 2.

The total electrical conductivity of a pure Na_2SO_4 melt and the melts containing various oxides was determined by measuring the resistance of the melts from the relation:

$$R = \left(\frac{1}{\sigma}\right) \text{Cell Constant} \qquad (3.1)$$

where R is the resistance measured in ohms, σ is the conductivity of the melt expressed in $(\text{ohm-cm})^{-1}$ and the cell constant is given in terms of cm^{-1}.

The cell constant, which is a characteristic of the conductivity cell, depends on the length between the electrodes and the surface area of the electrode exposed to the melt. The cell constant is usually predetermined by measuring the resistance across an ionic solution of known specific conductivity. Since the specific conductivity values of KCl solution are well established [23], an 0.1 N KCl solution was employed to determine the cell constant for the proposed work. The cell constant measurements were conducted at about 25°C utilizing identical cell arrangements with the gold crucible to contain an 0.1 N potassium chloride solution instead of the melt.

(iii) Wagner - Hebb Type Polarization Experiments

Wagner-Hebb type polarization technique was used to determine the partial electronic conductivities of a pure Na_2SO_4 melt and melts containing NiO as a function of Na_2O activity at 1173 K.

A constant voltage was supplied to the polarization cell via a Keithley 260 Nanovolt Source as shown in Figure 3. A Keithley Digital Multimeter, Model 177 was used as an ammeter. A Solid State Electrometer, Model 610C was utilized to check the actual voltage on the polarization cell.

Figure 4 shows the details of the polarization cell arrangements. Platinum wires were employed to lead gold electrodes into the power source and multimeter. Pure gold crucibles were used for these experiments. An A.C. impedance technique was utilized to determine the cell constant with the same cell geometry by measuring the conductivity of an 0.1 N KCl solution instead of the molten salts.

(iv) Potentiostatic Polarization Experiment

Most molten salts are ionic conductors. Thus, it seems logical to assume that molten sodium sulfate is an ionic conductor. The relative contributions of the different carrier species (cation vs. anion) was investigated by this technique.

A constant D.C. potential was applied via a Keithley 260 Nanovolt Source and the current was monitored by using a Keithley Digital Multimeter Model 177.

A symmetric cell configuration was employed and the electrode was chosen to match the cation in the molten sodium sulfate. The reversible electrode consists of a mullite tube conductive to sodium ions, containing a silver electrode immersed into a melt of Ag_2SO_4- 90 m/o Na_2SO_4. Mullite is a two-phase ceramic consisting of mullite grains ($3Al_2O_3$ - $2SiO_2$) enveloped by silica. At high temperatures dissolved alkali metal compounds in the silica film allow transport of alkali metal cations under an electrochemical driving force with essentially no electronic conduction [24,25].

IV. RESULTS and DISCUSSION

(i) Pure Na_2SO_4

The measured total electrical conductivities of a pure Na_2SO_4 at 1173 K are depicted in Figure 5 as a function of the activity of Na_2O in the melt. The total electrical conductivities remain rather constant regardless of the changes in Na_2O activities. The total electrical conductivity of a pure Na_2SO_4 melt was averaged as 0.257 $(ohm\text{-}cm)^{-1}$ which is about one order of magnitude smaller than the literature values [26-29]. This discrepancy is most probably caused by the facts that the previous investigators had: (1) a relatively impure Na_2SO_4, (2) a reaction between their quartz capillary and molten sodium sulfate, and (3) a reaction with their Pt electrodes. It was observed that there was significant deterioration of the quartz crucibles used to contain the Na_2SO_4 melts in our preliminary work and that there was a reaction of Na_2SO_4 melts with Pt electrodes initially utilized.

From the Wagner-Hebb type polarization measurements on pure Na_2SO_4 melt at 1173 K the partial conductivities of electrons and electron holes were obtained and are depicted in Figure 6. It can be seen that electron conduction in pure Na_2SO_4 is considerably larger than that of electron holes over the entire Na_2O activity range. Furthermore, it is noted that both electron and electron hole conductivities remain relatively constant regardless of the changes in Na_2O activities. Thus, the total electrical conductivity as well as partial electronic conductivities of a pure Na_2SO_4 melt are not dependent on the acidity and/or basicity of the melt.

From the measured values of total electrical conductivities and electronic conductivities, the transport numbers of electronic species may be computed. These numbers are plotted in Figure 7 for a pure Na_2SO_4 melt. The transport numbers of electrons are of the order of 10^{-4} while those of electron holes are of the order of 10^{-6}.

This indicates that the electronic conduction in a pure Na_2SO_4 melt arises primarily via electron transport over the whole Na_2O activity range. The transport numbers of electronic species in molten salts have not been measured extensively but the few that have been measured are somewhat larger than those determined in this study, e.g., $t_\theta = 3x10^{-3}$ in the molten eutectic of LiCl-KCl at 450°C [30].

(ii) Na_2SO_4 Melt Containing NiO

Ni based alloys have been used as construction materials for numerous applications at high temperatures. The simultaneous oxidation and hot corrosion of these alloys in SO_2 and O_2 gas mixture environments cause serious degradation of these materials. High temperature corrosion of Ni based alloys with gaseous SO_2 and O_2 have been well documented [31-38]. It is proposed that such serious degradation is due to the fluxing of protective oxide scales by the molten salts.

The present work was performed to assist in understanding the effect of NiO on the behavior of the electronic species in the melt in equilibrium with gaseous SO_2 and O_2. This work included measuring the total electrical conductivity by an A.C. impedance technique and conducting Wagner-Hebb type polarization experiments in the Na_2SO_4 melt containing NiO as a function of Na_2O activity at 1173 K.

The measured total conductivity of a pure Na_2SO_4 and the melts containing 10^{-3} m/o, 1.8×10^{-1} m/o, and supersaturated (10 m/o) NiO are shown in Figure 8 as a function of Na_2O activity at 1173 K. The total electrical conductivities remain rather constant regardless of the change in Na_2O activities and change in the amount of NiO in the melt. These results are somewhat contradictory to the proposed hot corrosion models [2-5] which describe the degradation behavior of the alloys as strongly dependent on the Na_2O activity in the molten sodium sulfate. Thus, efforts to check our previous results utilizing

certified SO_2/O_2 gas mixtures will be made on a pure Na_2SO_4 melt and the melts containing NiO. It is noted that the introduction of NiO into a Na_2SO_4 melt does not show massive changes in total electrical conductivities as compared to those of a pure Na_2SO_4 melt. These results indicate that the mobilities of the ions resulting from the dissolution of NiO are not significantly different from the ions present in the Na_2SO_4 melt. Thus, a phase stability diagram, constructed from the thermodynamic data, will be utilized to relate the responsible solute species to the electrical behavior of the molten salts. The choice of log P_{O_2} and log P_{SO_3} as coordinates for a phase stability plot has an advantage of explaining the possible species of metal oxides in the Na_2SO_4 melt as a function of the acidity of the melt.

The electronic conductivities observed for the melts containing NiO are shown in Figures 9 to 11. Basically, these results show that electron conductivities remain higher than the electron hole conductivities at all concentrations of NiO and throughout the entire range of Na_2O activities. Thus, the changes in acidity and/or basicity of the melt due to the introduction of NiO does not produce significant differences in partial electronic conductivities. However, the addition of NiO in molten Na_2SO_4 slightly decreases the electronic conductivities over the whole Na_2O activity range compared to those of a pure Na_2SO_4 melt. In addition, the results show an increase in electron conductivities in the low Na_2O activity region, especially for the melt containing supersaturated (10 m/o) NiO as shown in Figure 11. This behavior may relate to the dissolution products of NiO in the low Na_2O activity region.

Combining total electrical conductivities and partial electronic conductivities it is possible to calculate the transport numbers of electronic species in the melt with the additions of NiO. These results are plotted in Figures 12 to 14, for the melts containing 10^{-3} m/o, 1.8×10^{-1} m/o, and supersaturated (10 m/o) NiO, respectively. It can be seen that the transport numbers of electrons remain consistently higher than those of electron holes in accord with the partial and total electrical conductivities. These results imply that

the electrons are the major species contributing to the electronic conduction in such melts. It is noted that there is a significant increase in the transport numbers of electrons in the low Na_2O activity region in the melt containing supersaturated (10 m/o) NiO as shown in Figure 14. This resulted from the greater increase in electron conductivities than the increase in total electrical conductivities in this region.

(ii) Ionic Transport in Molten Salts

It is generally observed [39-41] that Na^+ ion conductivity prevails in solid Na_2SO_4 (235-883 C) and that the partial electronic conductivity is negligible. Thus the electrode for the potentiostatic polarization cell was chosen to be reversible with respect to the cation (Na^+) present in the molten sodium sulfate. If the cation reversible electrode works properly, then complete cell polarization is expected when the anion diffusion, created by a salt gradient, exactly opposes the migration of this ion under the influence of the applied potential.

Thus, cations in the melt are the only charge carriers and this was evidenced as a plateau in the current versus time curve as shown in Figure 15. The similar trends were observed at other sodium oxide activities in the melt and the cationic transport numbers of molten sodium sulfate were evaluated by dividing the final current, due to the cation only, by the initial current, due to the cation and anion.

The cationic transport numbers are displayed as a function of Na_2O activity in the melt in Figure 16. This result shows the cationic transport numbers are decreased as the sodium oxide activity of the melt are decreased. In another words, the contribution of the possible anion species such as SO_4^{--}, $S_2O_7^{--}$ and O^{--} increases as the acidity of the melt increases.

(iii) Final Remarks

The efforts on this proposal and by others [42] have shown that a number of possible steps in the hot corrosion process are not rate controlling. The diffusion in the gas phase boundary layer, chemical reaction at the gas phase/ Na_2SO_4 interface, diffusion in the boundary layer at the Na_2SO_4/ gas phase and diffusion in the bulk Na_2SO_4 are not major kinetic controlling steps. Thus, the chemical reaction at the liquid Na_2SO_4 / alloy interface could be a possible rate controlling step. To clarify which of the processes near the liquid Na_2SO_4 / alloy interface is rate controlling for the hot corrosion process, both conductivity and direct hot corrosion tests on Na_2SO_4 doped with $CaSO_4$ and Na_3VO_4 are under consideration.

V. SUMMARY AND CONCLUSION

The main thrust of this experimental program was to obtain some of the transport properties in the aggressive molten salt Na_2SO_4. The total electrical conductivity measurements by an A.C. impedance technique and Wagner-Hebb type polarization experiments provided the total electrical conductivity, electron conductivity, and electron hole conductivity of a pure Na_2SO_4 melt at 1173 K. From these measurements the transport numbers of electrons, $t_\ominus$, and electron holes, $t_\oplus$, were calculated as follows:

$$t_\ominus = 3.71 \times 10^{-4} ; \qquad t_\oplus = 6.95 \times 10^{-6}$$

Such experimental investigations show that the pure Na_2SO_4 melt had a somewhat low total electrical conductivity and the electronic conduction, which is somewhat lower than that of other molten salts, occurs primarily via the transport of electrons.

The effect of NiO on the electronic conduction as well as total electrical conductivity of the melt was examined by the same methods as applied to a pure Na_2SO_4 melt. The average values of the total electrical conductivities as well as partial electronic conductivities and their transport numbers are arranged in Tables 1 and 2, respectively. It is apparent from these tables that the addition of NiO does not change the total electrical conductivity significantly but decreases the electronic conductivities and the transport numbers of electronic species when compared to those of pure Na_2SO_4 melt, although there was a slight increase in partial electronic conductivities in a melt containing supersaturated (10 m/o) NiO, probably due to the dissolution product of NiO in the melt.

The cationic transport numbers of pure Na_2SO_4 melt was obtained by utilizing the potentiostatic polarization technique. The result indicates that the contribution of the anion species to the ionic current was not negligible especially in the acidic region of the melt.

Table 1. Average values of total electrical conductivities and partial electronic conductivities in a pure Na_2SO_4 melt and the melt containing NiO at 1173 K.

	Log σ	Log σ_θ^o	Log $\sigma_\oplus^o$
pure Na_2SO_4	-0.59	-4.03	-5.76
Na_2SO_4 with 10^{-3} m/o NiO	-0.64	-5.27	-6.34
Na_2SO_4 with 1.8×10^{-1} m/o NiO	-0.57	-5.82	-6.70
Na_2SO_4 with 10 m/o NiO	-0.76	-4.32	-5.94

Table 2. Average values of transport numbers of electronic species in a pure Na_2SO_4 melt and the melt containing NiO at 1173 K.

	t_θ	$t_\oplus$
pure Na_2SO_4	3.7×10^{-4}	7.0×10^{-6}
Na_2SO_4 with 10^{-3} m/o NiO	2.6×10^{-5}	2.3×10^{-6}
Na_2SO_4 with 1.8×10^{-1} m/o NiO	6.1×10^{-6}	8.2×10^{-7}
Na_2SO_4 with 10 m/o NiO	4.0×10^{-4}	8.4×10^{-5}

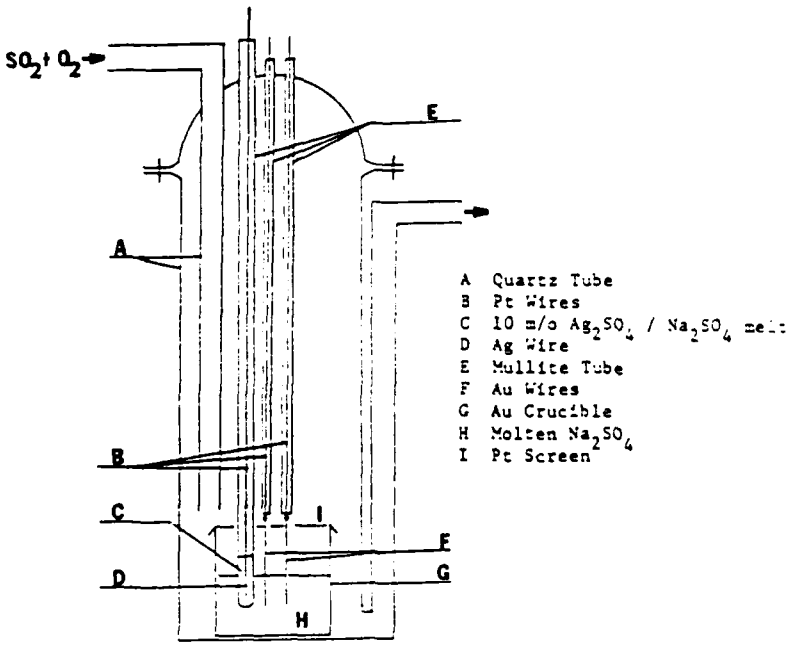

Figure 1. Schematic A.C. impedance cell arrangement

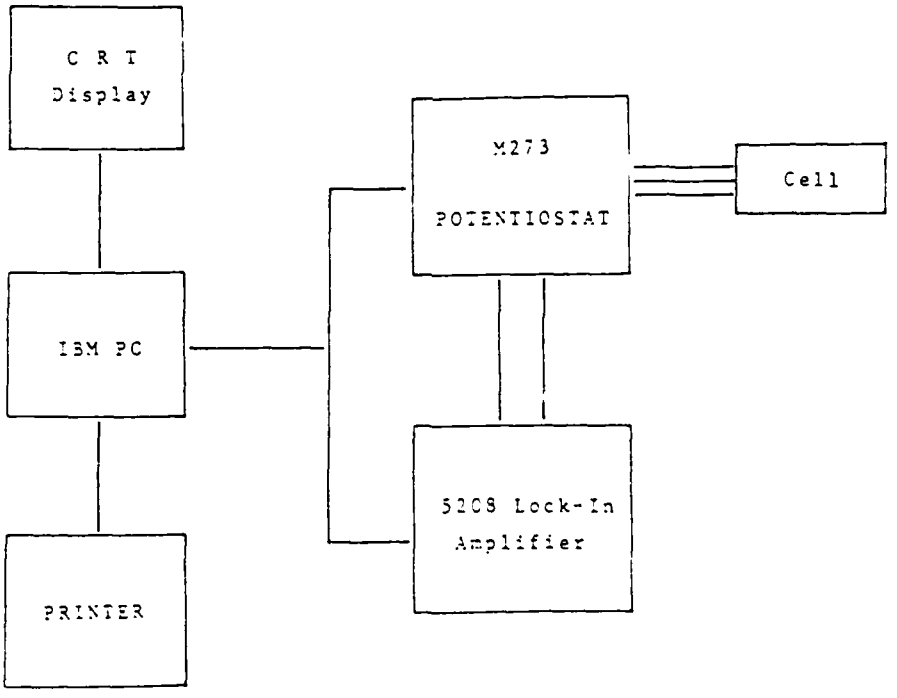

Figure 2. Schematic diagram of A.C. impedance experiment

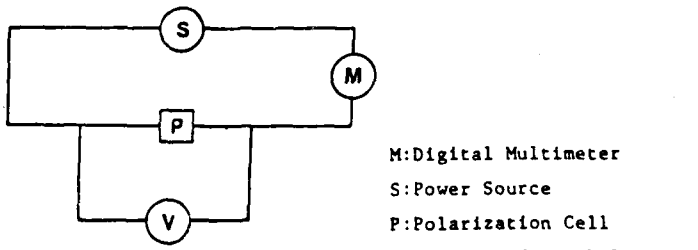

Figure 3. Schematic circuit diagram for Wagner-Hebb type polarization experiment

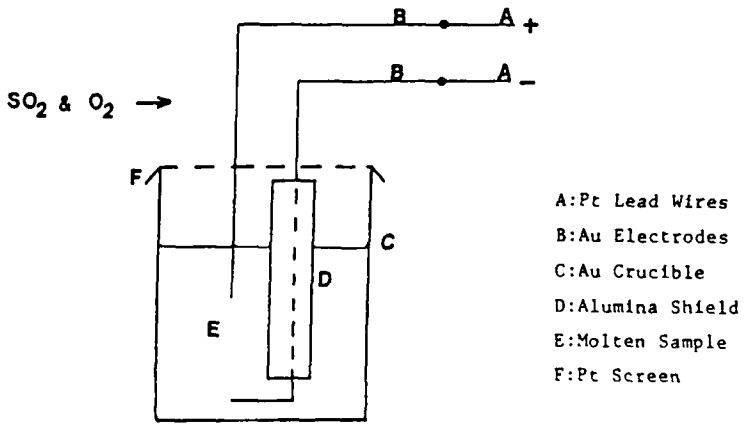

Figure 4. Wagner-Hebb type polarization cell arrangement

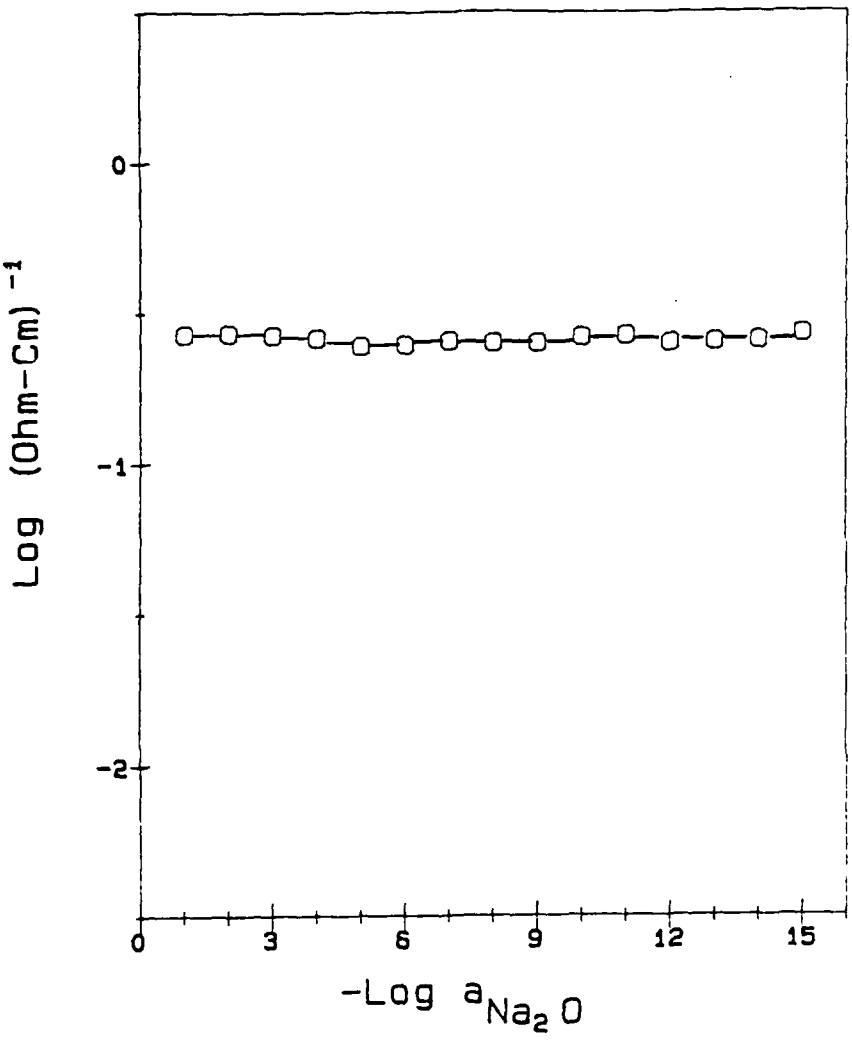

Figure 5. Log (total conductivity) versus Na_2O activity in a pure Na_2SO_4 melt at 1173 K

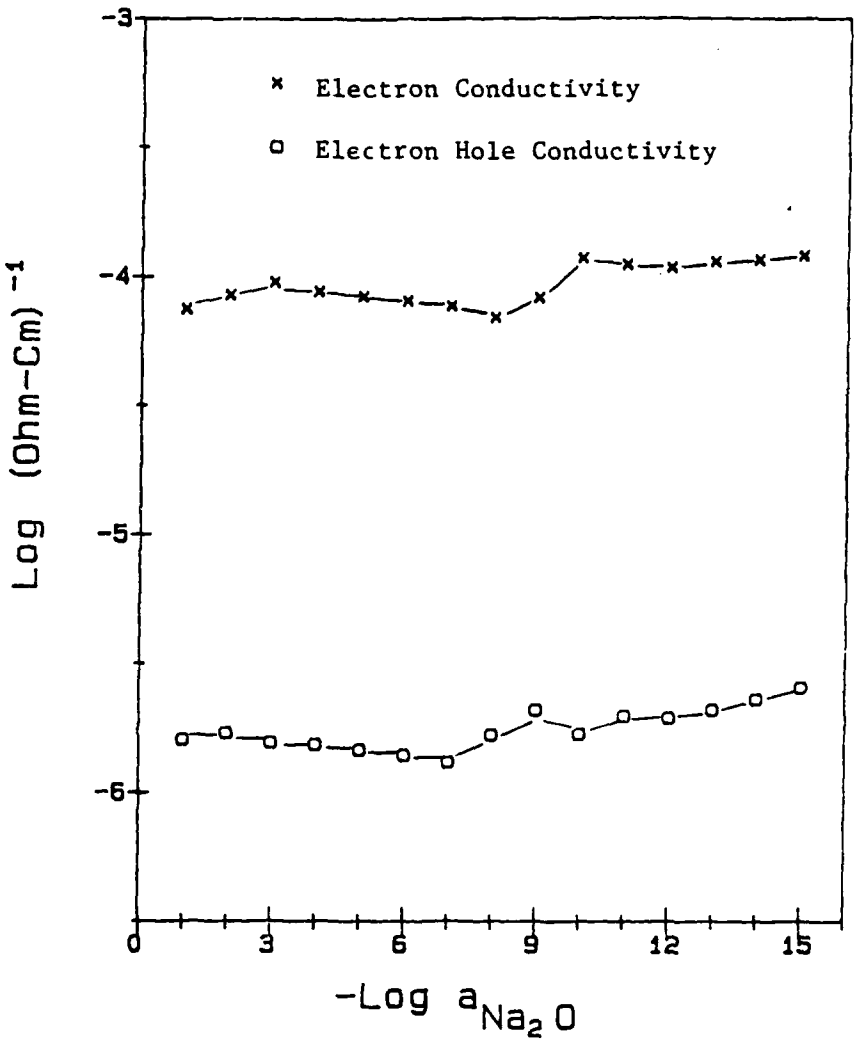

Figure 6. Electronic conductivities in a pure Na_2SO_4 melt as a function of Na_2O activity at 1173 K

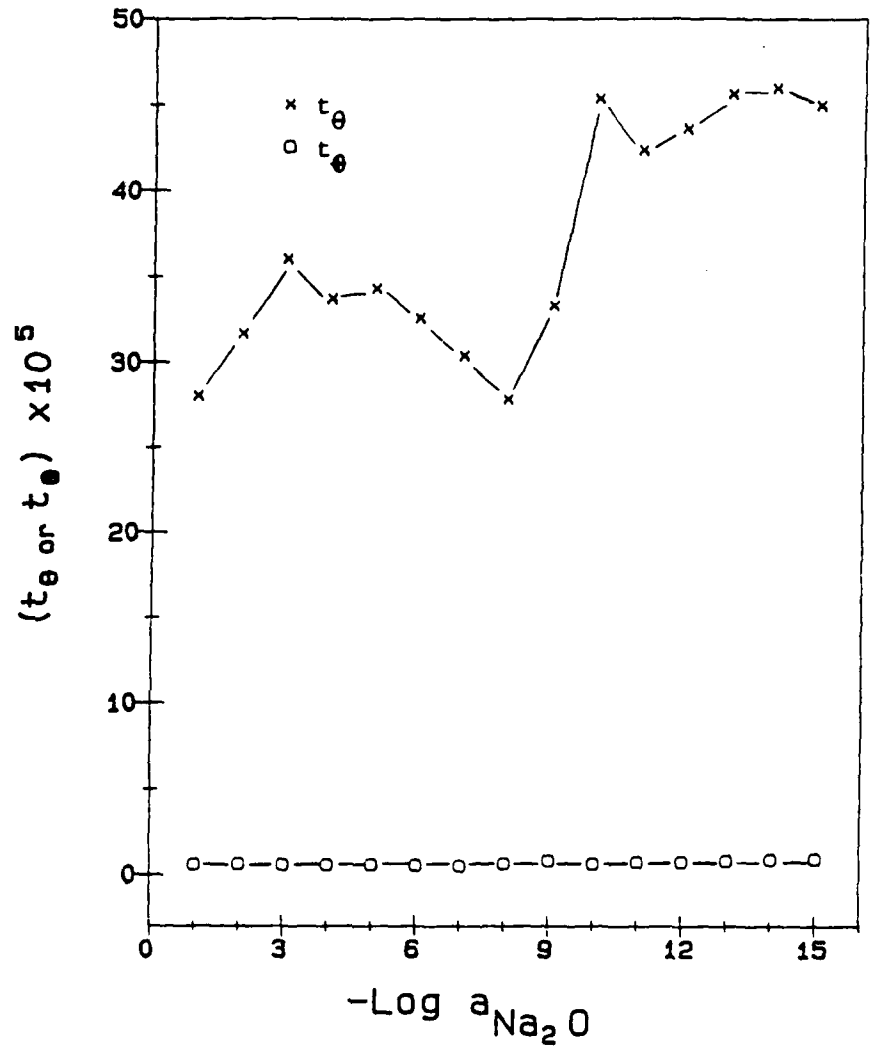

Figure 7. Transport numbers of electronic species in a pure Na_2SO_4 melt as a function of Na_2O activity at 1173 K

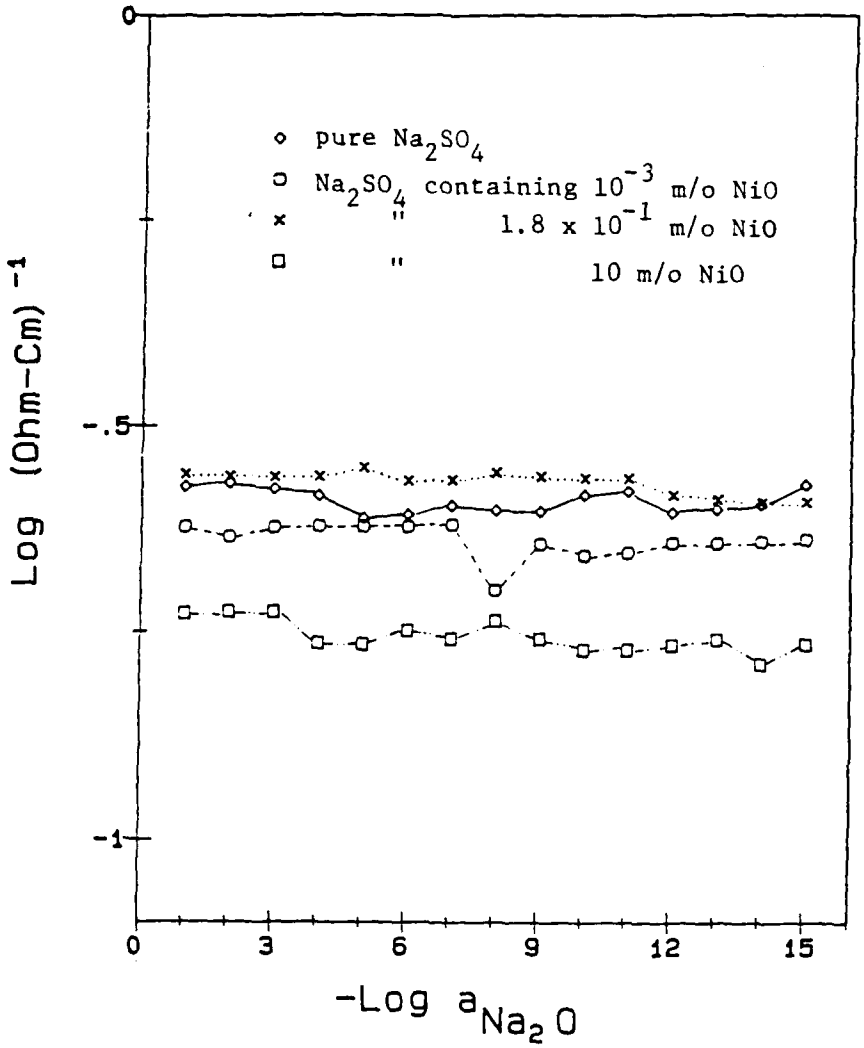

Figure 8. Log (total conductivity) versus Na_2O activity in a Na_2SO_4 melt containing 10^{-3} m/o, 1.8×10^{-1} m/o, and supersaturated (10 m/o) NiO at 1173 K

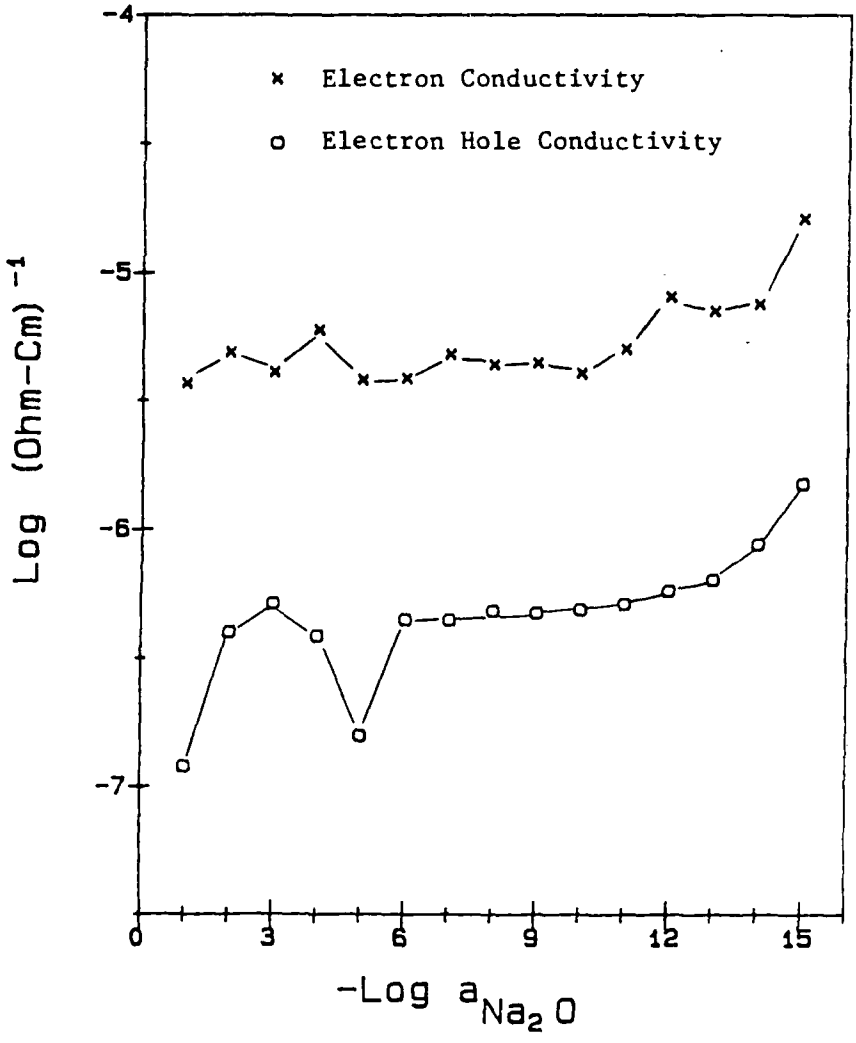

Figure 9. Electronic conductivities in a Na_2SO_4 melt with the addition of 10^{-3} m/o NiO as a function of Na_2O activity at 1173 K

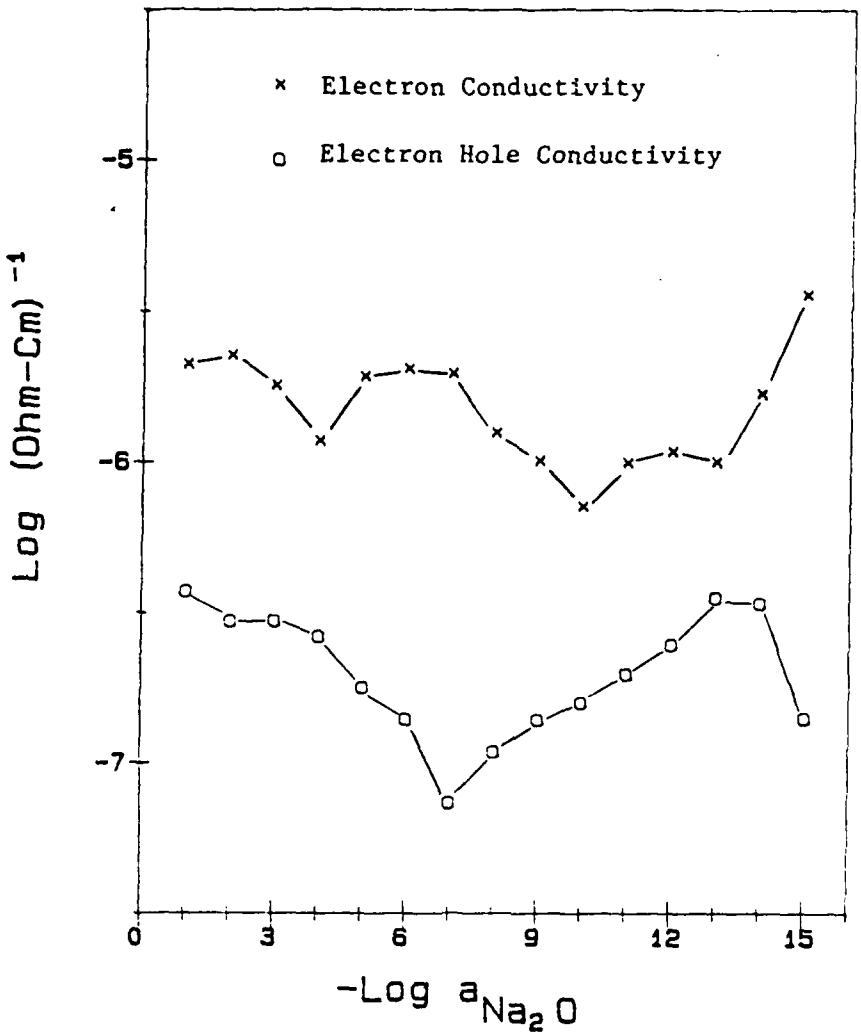

Figure 10. Electronic conductivities in a Na_2SO_4 melt with the addition of 1.8×10^{-1} m/o NiO as a function of Na_2O activity at 1173 K

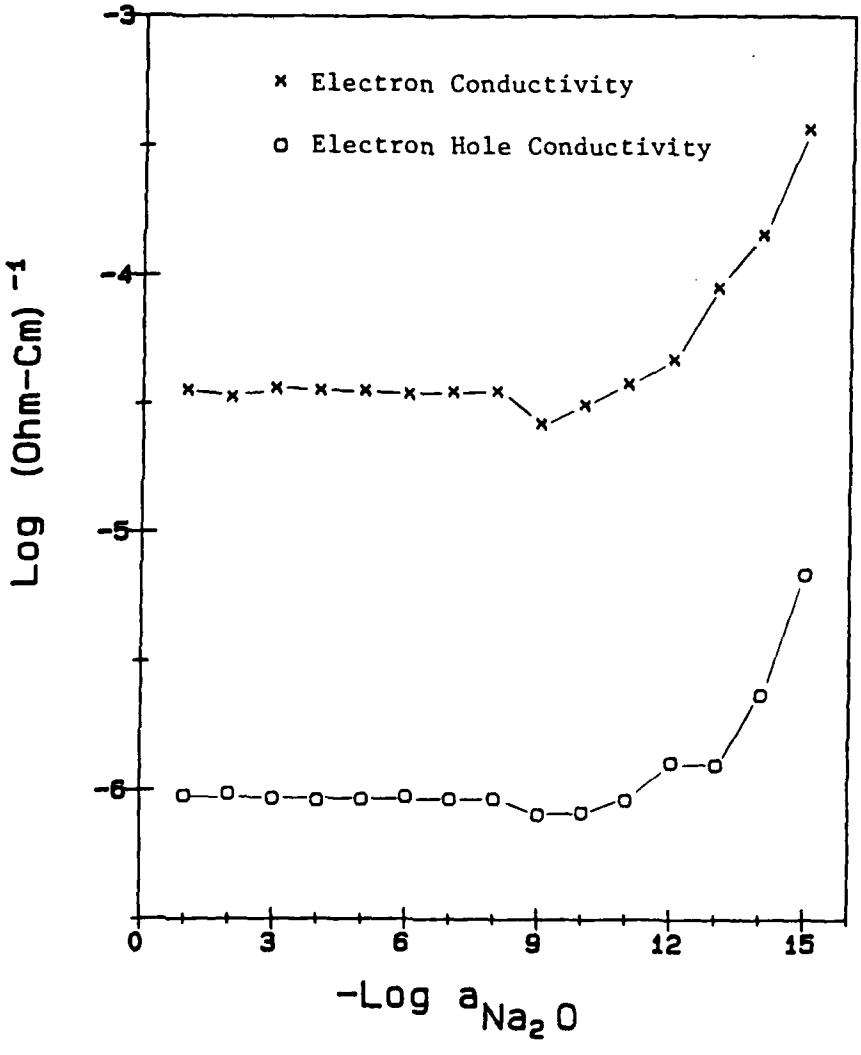

Figure 11. Electronic conductivities in a Na_2SO_4 melt with supersaturated (10 m/o) NiO as a function of Na_2O activity at 1173 K

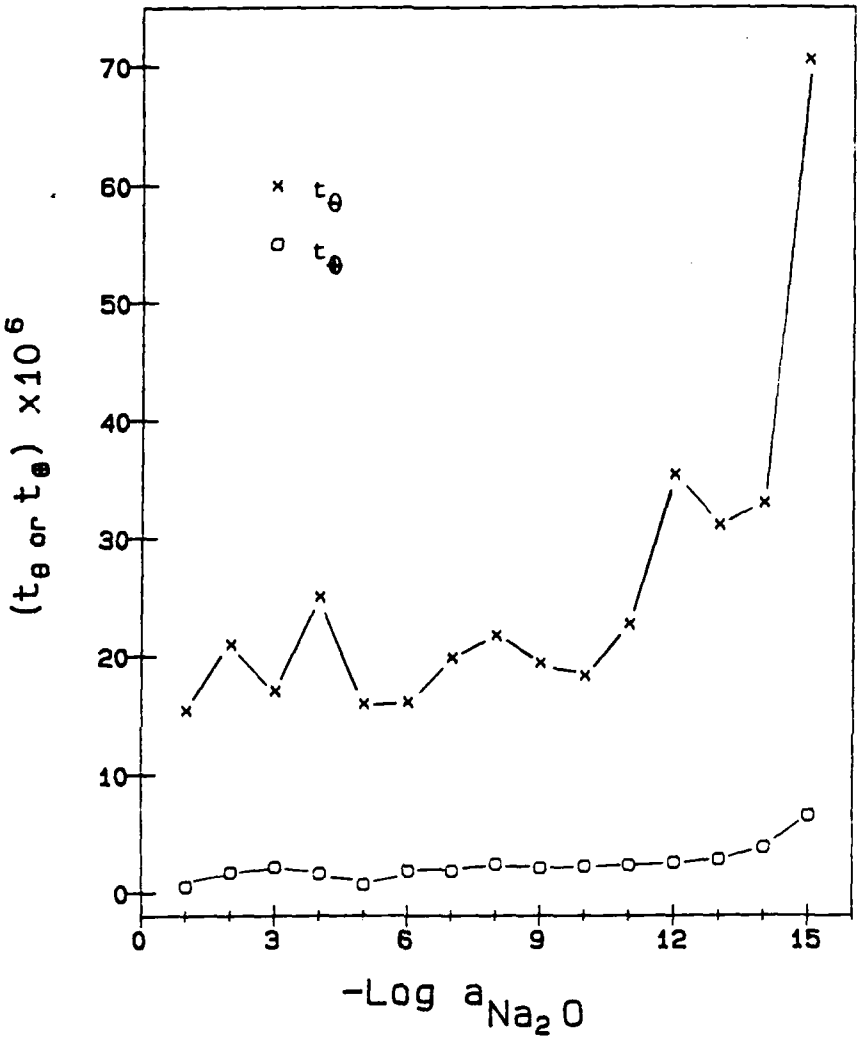

Figure 12. Transport numbers of electronic species in molten Na_2SO_4 containing 10^{-3} m/o NiO at 1173 K

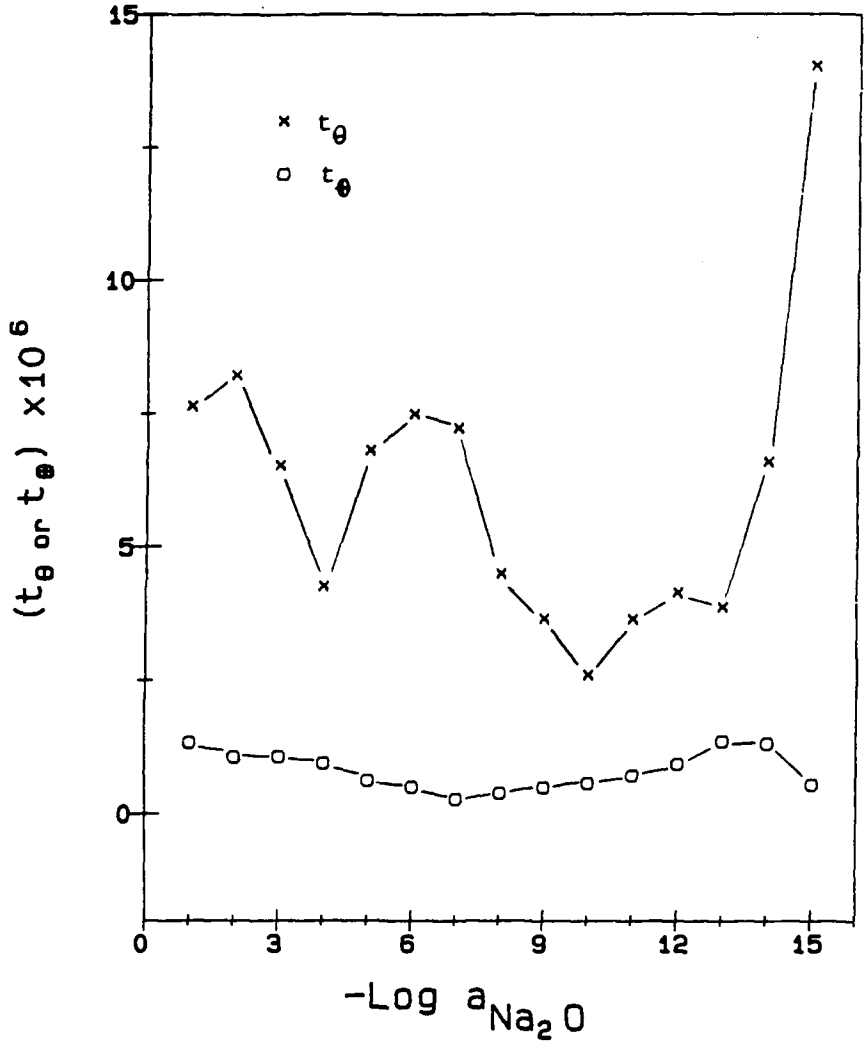

Figure 13. Transport numbers of electronic species in molten Na_2SO_4 containing 1.8×10^{-1} m/o NiO at 1173 K

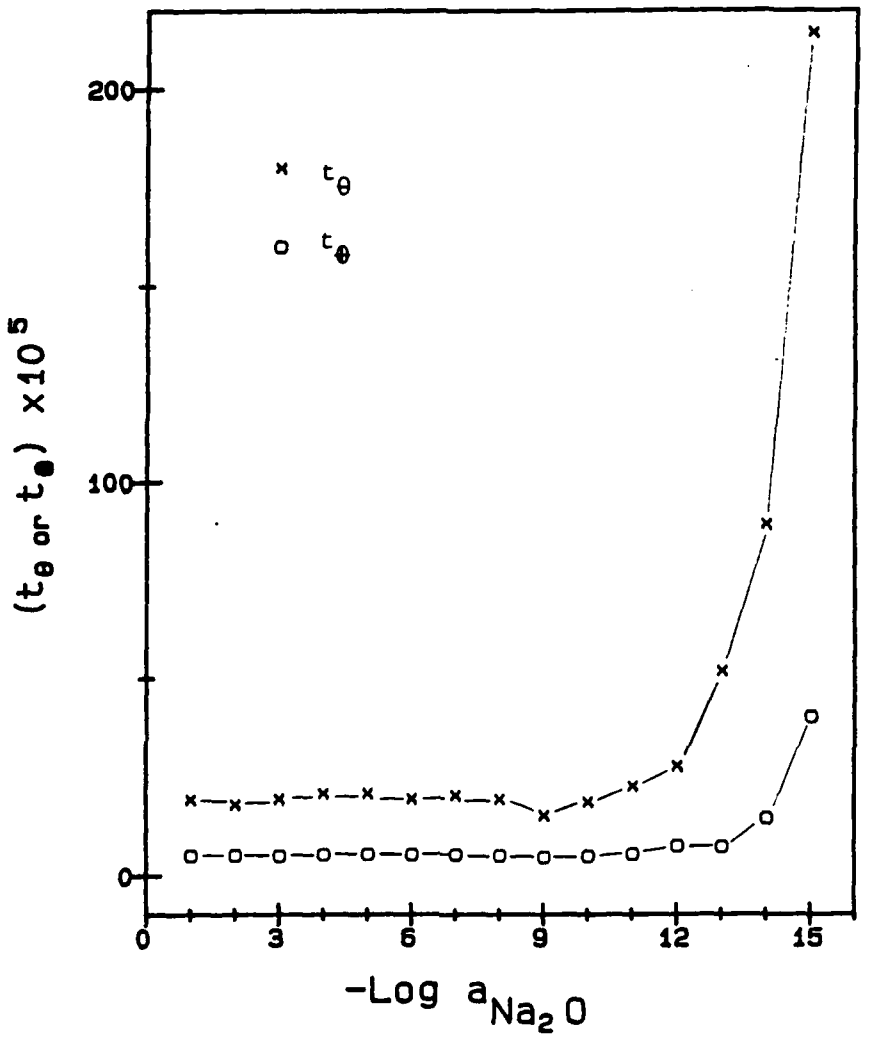

Figure 14. Transport numbers of electronic species in molten Na_2SO_4 containing supersaturated (10 m/o) NiO at 1173 K

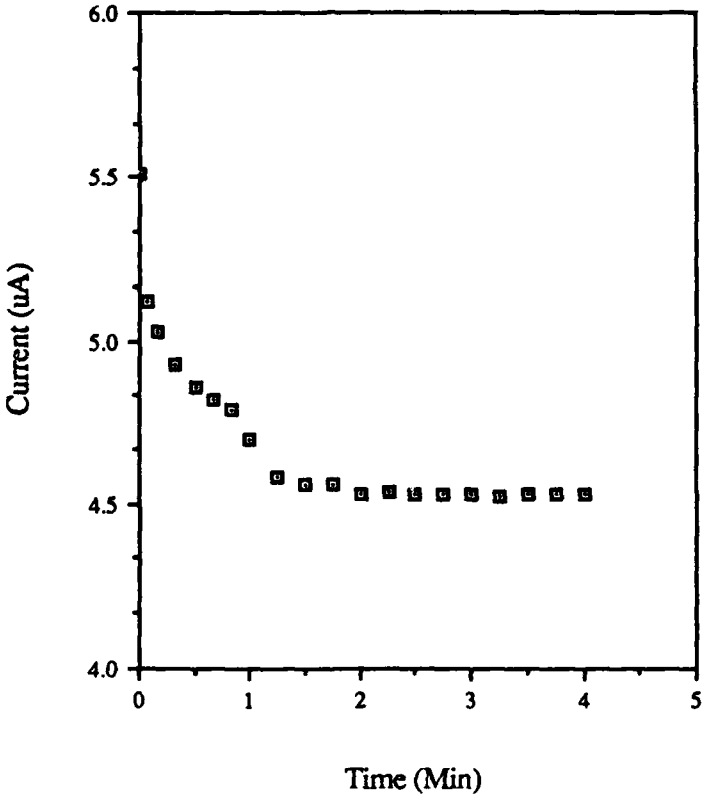

Figure 15. Current versus time plot for the melt at -log (Na_2O activity) equals to 14 at 1173 K.

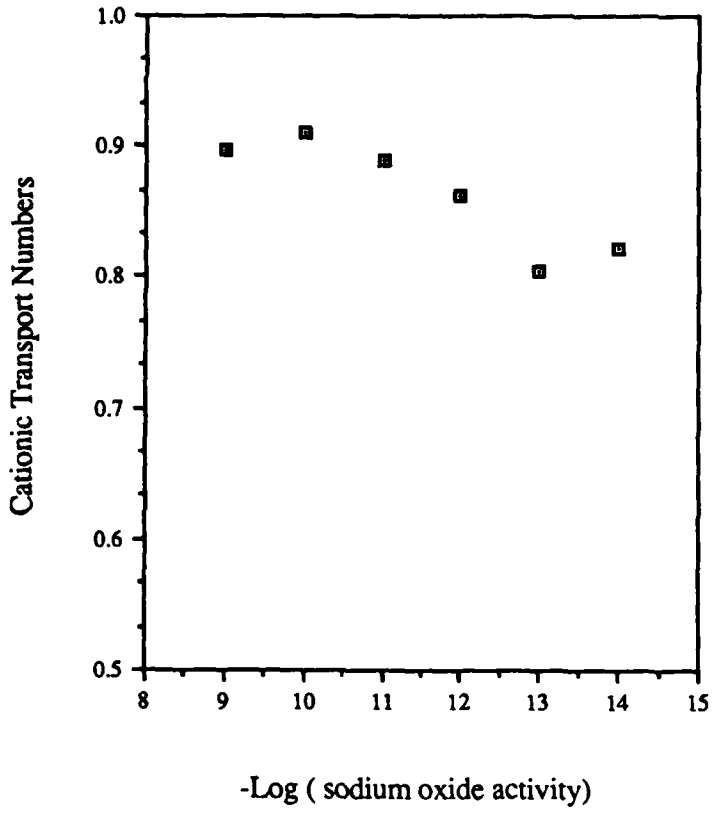

Figure 16. Cationic transport numbers of the Na_2SO_4 melt as a function of Na_2O activity at 1173 K

REFERENCES

1. J.M. Quets and W.H. Dresher, Nuc. Mat., 14, 583 (1969)
2. N.S. Bornstein, M.A. DeCrescente, Met. Trans., 2, 2875 (1971)
3. J.A. Goebel and F.S. Pettit, Met. Trans.,1, 1943 (1970)
4. J.A. Goebel, F.S. Pettit, and G.W. Goward, Met. Trans., 4 , 261 (1973)
5. R.A. Rapp and K.S. Goto, "Proceedings of Second International Symposium on Molten Salts", J.Braunstein and J.R. Selman eds., Electrochem. Soc. p159 (1981)
6. C. Wagner, Proc. of Seventh Meeting of the Inter. Comm. on Thermo. and Kinetics of Electrochem. (CITCE), Butterworth Scientific Publications, London, Vol. 7, p. 361 (1957).
7. M. H. Hebb, J. Chem. Phys., 20, 185 (1952).
8. J.E.B. Randles, Dis. Faraday. Soc., 1, 11 (1947)
9. G.W. Walter, Corr. Sci., 26, 681 (1986)
10. F. Mansfeld, Corr.-NACE, 36, 301 (1981).
11. J. B. Wagner, Jr. and C. Wagner, J. Chem. Phys., 26, 1597 (1957).
12. A. Lingras and G. Simkovich, J. Phys. Chem. Solids, 39, 1225 (1978).
13. A. V. Joshi and J. B. Wagner, Jr., J. Phys. Chem. Solids, 33, 205 (1972).
14. A. V. Joshi and J. B. Wagner, Jr., J. Electrochem. Soc., 122, 1071 (1975).
15. D. Raleigh, J. Phys. Chem. Solids, 26, 329 (1965).
16. J. Sachoonman, A. Wolfert, and D. F. Untereker, Solid State Ionics, 11, 187 (1983).
17. R. J. Heus and J. J. Egan, J. Phys. Chem., 77, 1989 (1973).
18. R. J. Heus and J. J. Egan, in "Proceedings of International Symposium on Molten Salts," Electrochem. Soc., Pennington, NJ (1976), p. 523.

19. G. J. Reynolds, M.C.Y. Lee and R. A. Huggins, in "Proceedings of the Fourth International Symposium on Molten Salts," Electrochem. Soc., pv 84-2, Pennington, NJ (1984), p. 519.

20. D.F. Shriver, S. Clancy, P.M. Blonsky, and L.C. Hardy, "Sixth Risφ International Symposium on Met. and Mat. Sci." p353 (1985)

21. D.H. Kim and G. Simkovich, "Proceedings of Symposium on High Temperature Materials Chemistry IV", Ed. Z.A. Munir, D. Cubicciotti, and H. Tagawa, Electrochem Soc. 88-5, p26 (1988)

22. D. A. Shores and R. C. John, J. Appl. Electrochem. 10, 275 (1980).

23. D. Dobos, "Electrochemical Data," Elsevier Scientific Publishing Co., New York, p. 57 (1975).

24. R.J. Labrie and V.A. Lamb, J. Electrochem. Soc., 106, 895 (1959)

25. H. Schmalzreid, Z. Phys. Chem. (Frankfurt), 38, 87 (1963)

26. A. Kvist, Z. Naturforschg., 22a, 208 (1967).

27. A. Kvist, Z. Naturforschg., 22a, 467 (1967).

28. A. Josefson and A. Kvist, Z. Naturforsch, 24a, 466 (1969).

29. K. Matiasovsky, V. Danek, and B. Lillebuen, Electrochim. Acta, 17, 463 (1972).

30. R. J. Heus and J. J. Egan, J. Phys. Chem., 77, 1989 (1973).

31. V. Vasantasree and M. G. Hocking, Corr. Sci., 16, 261 (1976).

32. P. Kofstad and G. Åkesson, Oxid. Met., 12, 503 (1979).

33. K. L. Luthra and W. L. Worrell, Met. Trans., 9A, 1055 (1978).

34. C. B. Alcock, M. G. Hocking and S. Zador, Corr. Sci., 9, 111 (1969).

35. P. Kofstad and G. Åkesson, Oxid. Met., 14, 301 (1980).

36. A. K. Misra and D. P. Whittle, Oxid. Met., 22, 1 (1984).

37. R. F. Reising and D. P. Krause, Corr.-NACE, 30, 131 (1974).

38. K. P. Lillerud and P. Kofstad, Oxid. Met., 21, 233 (1984).

39. K. Shahi and G. Prakash, Solid State Ionics 18 & 19, 544 (1986)

40. H.H. Hofer, W. Eysel and U.V. Alpen, Mater. Res. Bull., 13,265 (1978)

41. K.T. Jacob and D.B. Rao, J. Electrochem. Soc., 126, 1842 (1979)

42. J.S. Patton, MS Thesis, PSU (1988)

BASIC DISTRIBUTION LIST

Technical and Summary Reports 1988

Organization	Copies
Defense Documentation Center Camerson Station Alexandria, VA 22314	12
Office of Naval Research Dept. of the Navy 800 N. Quincy Street Arlington, VA 22217 Attn: Code 1131	3
Naval Research Laboratory Washington, DC 20375 ATTN: Codes 6000 6300 2627	
Naval Air Development Center Code 606 Warminister, PA 18974 ATTN: Dr. J. DeLuccia	
Commanding Officer Naval Surface Weapons Center White Oak Laboratory Silver Spring, MD 20910 ATTN: Library	1
Naval Oceans Systems Center San Diego, CA 92132 ATTN: Library	1
Naval Postgraduate School Monterey, CA 93940 ATTN: Mechanical Engineering Department	1
Naval Air Systems Command Washington, DC 20360 Attn: Code 310A Code 5304B Code 931A	1 1 1
Naval Sea System Command Washington, DC 20362 ATTN: Code 05M Code 05R	1 1
Naval Air Prop. Test Ctr. Trenton, NY 08628 ATTN: Library	1
Naval Contruction Battallion Civil Engineering Laboratory Port Hueneme, CA 93043 ATTN: Materials Div.	1
Naval Electronics Laboratory San Diego, CA 92152 ATTN: Electron Materials Sciences Division	1
Naval Missile Center Materials Consultant Code 3312-1 Point Mugu, CA 92041	1
Commander David Taylor Research Center Bethesda, MD 20084	1
Naval Underwater System Ctr. Newport, RI 02840 ATTN: Library	1
Naval Weapons Center China Lake, CA 93555 ATTN: Library	1
NASA Lewis Research Center 21000 Brookpark Road Cleveland, OH 44135 ATTN: Library	1
National Bureau of Standards Gaithersburg, MD 20899 Attn: Metallurgy Division Ceramics Division Fracture & Deformation Division	1 1 1

Naval Facilities Engineering
Command
Alexandria, VA 22331
ATTN: Code 03 1

Scientific Advisor
Commandant of the Marine Corps
Washington, DC 20380
ATTN: Code AX 1

Army Research Office
P.O. Box 12211
Research Triangle Park, NC 27709
ATTN: Metallurgy & Ceramics
Program 1

Army Materials and Mechanics
Research Center
Watertown, MA 02172
ATTN: Research Programs Office 1

Air Force Office of Scientific
Research/NE
Building 410
Bolling Air Force Base
Washington, DC 20332
ATTN: Electronics & Materials
Science Directorate 1

NASA Headquarters
Washington, DC 20546
Attn: Code RM 1

Defense Metals & Ceramics
Information Center
Battelle Memorial Inst.
505 King Avenue
Columbus, OH 43201 1

Metals and Ceramics Div.
Oak Ridge National Laboratory
P.O. Box X
Oak Ridge, TN 37380 1

Los Alamos Scientific Lab.
P.O. Box 1663
Los Alamos, NM 87544
ATTN: Report Librarian 1

Argonne National Laboratory
Metallurgy Division
P.O. Box 229
Lemont, IL 60439 1

Brookhaven National Laboratory
Technical Information Division
Upton, Long Island
New York 11973
Attn: Research Library 1

Lawrence Radiation Lab.
Library
Building 50, Room 134
Berkely, CA 1

David Taylor Research Ctr
Annapolis, MD 21402-5067
ATTN: Code 281 1
Code 2813 1
Code 0115 1

RE/1131/88/75
4315 (036)

Supplemental Distribution List Feb 1988

Prof. I.M. Bernstein
Illinois Institute of Technology
IIT Center
Chicago, Ill 60615

Prof. H.K. Birnbaum
Dept. of Metallurgy & Mining Eng.
University of Illinois
Urbana, Ill 61801

Prof. H.W. Pickering
Dept. of Materials Science and Eng.
The Pennsylvania State University
University Park, PA 16802

Prof. D.J. Duquette
Dept. of Metallurgical Eng.
Rensselaer Polytechnic Inst.
Troy, NY 12181

Prof. J.P. Hirth
Dept. of Metallurgical Eng.
The Ohio State University
116 West 19th Avenue
Columbus, OH 43210-1179

Prof. H. Leidheiser, Jr.
Center for Coatings and Surface Research
Sinclair Laboratory, Bld. No. 7
Lehigh University
Bethlehem, PA 18015

Dr. M. Kendig
Rockwell International Science Center
1049 Camino Dos Rios
P.O. Box 1085
Thousand Oaks, CA 91360

Prof. R. A. Rapp
Dept. of Metallurgical Eng.
The Ohio State University
116 West 19th Avenue
Columbus, OH 43210-1179

Profs. G.H. Meier and F.S.Pettit
Dept. of Metallurgical and
Materials Eng.
University of Pittsburgh
Pittsburgh, PA 15261

Dr. W. C. Moshier
Martin Marietta Laboratories
1450 South Rolling Rd.
Baltimore, MD 21227-3898

Prof. P.J. Moran
Dept. of Materials Science & Eng.
The Johns Hopkins University
Baltimore, MD 21218

Prof. J. Kruger
Dept. of Materials Science & Eng.
The Johns Hopkins University
Baltimore, MD 21218

Prof. R.P. Wei
Dept. of Mechanical Engineering
and Mechanics
Lehigh University
Bethlehem, PA 18015

Prof. W.H. Hartt
Department of Ocean Engineering
Florida Atlantic University
Boca Raton, Florida 33431

Dr. B.G. Pound
SRI International
333 Ravenswood Ave.
Menlo Park, CA 94025

Prof. C.R. Clayton
Department of Materials Science
& Engineering
State University of New York
Stony Brook
Long Island, New York 11794

Prof. Boris D. Cahan
Dept. of Chemistry
Case Western Reserve Univ.
Cleveland, Ohio 44106

Dr. K. Sadananda
Code 6323
Naval Research Laboratory
Washington, D.C. 20375

Prof. M.E. Orazem
Dept. of Chemical Engineering
University of Virginia
Charlottesville, VA 22901

Dr. G.R. Yoder
Code 6384
Naval Research Laboratory
Washington, D.C. 20375

Dr. N. S. Bornstein
United Technologies Research Center
East Hartford, CT 06108

Dr. A.L. Moran
Code 2812
David Taylor Research Center
Annapolis, MD 21402-5067

Dr. B.E. Wilde
Dept. of Metallurgical Engineering
The Ohio State University
116 West 19th Avenue
Columbus, OH 43210-1179

Prof. G.R. St. Pierre
Dept. of Metallurgical Eng.
The Ohio State University
116 West 19th Avenue
Columbus, OH 43210-1179

Prof. G. Simkovich
Dept. of Materials Science & Eng.
The Pennsylvania State University
University Park, PA 16802

Dr. E. McCafferty
Code 6322
Naval Research Laboratory
Washington, D. C. 20375

Dr. J.A. Sprague
Code 4672
Naval Research Laboratory
Washington, D.C. 20375

Dr. C.M. Gilmore
The George Washington University
School of Engineering & Applied Science
Washington, D.C. 20052

Dr. F.B. Mansfeld
Dept. of Materials Science
University of Southern California
University Park
Los Angeles, CA 90089

Dr. Ulrich Stimming
Dept. of Chemical Eng. & Applied Chemistry
Columbia University
New York, N.Y. 10027

Prof. J. O'M. Bockris
Dept. of Chemistry
Texas A & M University
College Station, TX 77843